Redox behavior of supported Pd particles and its effect on oxygen reduction reaction in intermediate temperature solid oxide fuel cells

Fengli Liang[a], Jing Chen[a], Bo Chi[a,*], Jian Pu[a], San Ping Jiang[b], Li Jian[a]

[a] School of Materials Science and Engineering, State Key Laboratory of Material Processing and Die & Mould Technology, Huazhong University of Science and Technology, Luoyu Rd 1037, Wuhan, Hubei 430074, PR China
[b] School of Mechanical and Aerospace Engineering, Nanyang Technological University, Singapore 639798, Singapore

ABSTRACT

Nano-structured Pd-infiltrated YSZ cathodes (Pd + YSZ) are prepared by impregnation method and their electrocatalytic activity and reduction–oxidation behavior are investigated. It is observed that nano-sized PdO particles are uniformly distributed on the surface of the YSZ scaffold and decomposed at a temperature below 800 °C in air. Coexistence of Pd and PdO in the Pd + YSZ cathode is detected at temperatures between 650 and 750 °C. The polarization resistance R_E of the Pd + YSZ cathode decreases continuously as oxygen partial pressure increases from 0.001 to 1 atm at 600 and 850 °C, whereas it reaches a minimum in the vicinity of 0.03 atm of oxygen partial pressure at 750 °C. In air with an oxygen partial pressure of 0.21 atm, the Pd + YSZ shows the lowest activation energy for the oxygen reduction reaction in the temperature range of 650 and 750 °C.

© 2010 Elsevier B.V. All rights reserved.

1. Introduction

Solid oxide fuel cells (SOFCs) are a kind of high temperature electrochemical device that converts the chemical energy stored in fossil or hydrocarbon fuels to electricity efficiently beyond the limit of the Carnot cycle, with high quality heat as the byproduct. Thus, for the same amount of electricity generated, the level of pollutant and greenhouse gas emission from SOFCs is much lower than that from conventional power generation technologies. From both technical and commercial perspectives, it is desirable to reduce the operating temperature of SOFCs from the conventional high temperature range near 1000 °C to the intermediate temperature range between 600 to 800 °C; low-cost alloys may then be readily used as the interconnects [1]. However, reduction in operating temperature significantly increases the electrode polarization loss, especially at the cathode for oxygen reduction [2,3]. Thus, the development of high performance cathodes is of critical importance for the successful application of intermediate temperature SOFCs (IT-SOFCs).

Wet impregnation is an effective method to introduce nano-sized and catalytic active particles into porous scaffolds to form functional composite electrodes of SOFCs, dramatically enhancing their performance and avoiding the difficulties encountered in preparation of composite electrodes by conventional powder mixing and sintering. Recently, the wet impregnation method has attracted greater attention, and its global development has been thoroughly reviewed by Jiang [4] and Vohs and Gorte [5]. Impregnation of electrolyte particles into porous structure of perovskite catalysts [6,7] or vice versa [8] has been proven to substantially reduce the cathodic polarization resistance of the cathodes. Impregnations of noble metals into SOFC cathodes, such as Pt [9–11], Pd [11,12] or Ag [11,13], have also been investigated in terms of the effectiveness on cathode performance, and Pd has been confirmed beneficial in enhancing the oxygen reduction reaction occurred on various kinds of cathodes. More recently, detailed studies have been carried out by Liang et al. [14–16] on the role of Pd as a catalyst or a cathode promoter for oxygen reduction in SOFCs. It has found that solution-impregnated nano-sized Pd particles on the scaffold of Y_2O_3 stabilized ZrO_2 (YSZ) is an effective cathode with a polarization resistance as low as $0.22\,\Omega\,cm^2$ at 700 °C [16], and its performance can be stabilized by 5 wt.% Mn substitution for Pd [17]. And the electrochemical performance of Pd-promoted LSM-based cathodes was significantly improved; a considerably low electrode polarization resistance of $0.9\,\Omega\,cm^2$ at 600 °C was achieved, in contrast to $70\,\Omega\,cm^2$ obtained at the same temperature from the conventional LSM-YSZ cathode [15,16].

In the present study, the Pd-impregnated YSZ composite cathode (Pd + YSZ) was further investigated using techniques of high temperature X-ray diffraction and electrochemical impedance

* Corresponding author. Tel.: +86 27 87557694; fax: +86 27 87558142.
E-mail address: chibo@hust.edu.cn (B. Chi).

spectroscopy, aiming to identify the mechanisms for the enhancement on oxygen reduction in this type of cathode under intermediate temperature SOFC operating conditions.

2. Experimental

Dense electrolyte substrates with a dimension of ϕ 21 mm × 1 mm were fabricated from 8 mol% YSZ (TZ8Y, Tosoh, Japan) by die-pressing at room temperature and then sintering at 1500 °C for 4 h in air. To form a porous YSZ scaffold that hosts the impregnated species on the dense electrolyte substrates, YSZ slurry was made by mixing YSZ powder and organic binder, which was then screen-printed on the top surface of the dense electrolyte substrates and heat-treated at 1200 °C for 1 h in air. In order to construct functional Pd-impregnated YSZ cathodes (Pd + YSZ), the Pd-containing solution was prepared by dissolving $PdCl_2$ in diluted hydrochloric acid and infiltrated dropwise into the porous YSZ scaffold, followed by firing at 750 °C in air for 1 h. PdO particles were formed on the surface of the porous YSZ structure after the heat treatment. Detail preparation of the Pd + YSZ cathode was described in Ref. [14]. The thickness and area of the prepared cathode were 10–20 μm and 0.5 cm^2, respectively. The PdO content in the Pd + YSZ cathodes was estimated to be around 5 wt.% after 7 consecutive impregnations.

For electrochemical evaluation of the Pd + YSZ cathodes, Pt paste was painted on the opposite side of the working electrode and subsequently baked at 800 °C in air for 30 min to form the counter (0.5 cm^2) electrode and circular reference electrode. The gap between the counter electrode and reference electrode was 4 mm, ensuring that this distance was at least three times more than the thickness of the electrolyte to meet the extreme measurement requirement in the three-electrode configuration [18]. Pt mesh was used as the current collector; and electrochemical impedance spectra at open circuit were obtained at temperatures between 600 and 850 °C after soaking for 30 min at the measuring temperature in various controlled atmospheres consisting of N_2 and O_2, using an impedance/gain phase analyzer (Solartron 1260) and an electrochemical interface (Solartron 1287) in a frequency range from 0.1 to 100 kHz. The amplitude of the signal was 10 mA and 2 min were needed for a single impedance spectrum measurement. The total gas flow rate was 100 mL min^{-1} with N_2 and O_2 each controlled by a mass flow meter.

The phase change with temperature in the cathode was characterized by X-ray diffraction (XRD) using an X-ray diffractometer (X'Pert PRO Holand PANalytical B.V. Company) fitted with a high temperature specimen holder. The high temperature XRD was conducted in air during heating and cooling between room temperature and 900 °C after soaking 15 min at each testing temperature. A scanning electronic microscope (SEM, Sirion 200 Holand FEI Company) was employed for microstructure examinations of the cathodes.

3. Results and discussion

3.1. Reduction–oxidation of supported PdO nanoparticles

For unsupported PdO particles, the reduction–oxidation (redox) process of PdO was found to consist of two steps. During heating, PdO decomposes at the decomposition temperature T_d to form Pd with a sharp weight loss; and upon cooling, Pd re-oxidizes to PdO at the temperature T_R with a weight gain, usually below 800 °C. The redox reaction can be expressed as

$$Pd + \frac{1}{2}O_2 \Leftrightarrow PdO \tag{1}$$

with an equilibrium constant K_p as follow

$$K_p = \frac{1}{(P_{O_2})^{1/2}} \tag{2}$$

Rearranging above gives,

$$P_{O_2} = \left(\frac{1}{K_P}\right)^2 \tag{3}$$

where P_{O_2} is the decomposition pressure of PdO. The relationship between equilibrium constant K_p and temperature (T) is given by:

$$K_p = \exp\left(-\frac{\Delta G(T)}{RT}\right) \tag{4}$$

where R is the gas constant and $\Delta G(T)$ the formation free energy of PdO. Using the data provided in Ref. [19], $\Delta G(T)$ can be approximately expressed as

$$\Delta G(T) = -111,261 + 96.67T \tag{5}$$

Substituting Eq. (5) to Eq. (4) and then Eq. (4) to Eq. (3) gives,

$$P_{O_2} = \left(\frac{1}{\exp(-111,261 + 96.67T/RT)}\right)^2 \tag{6}$$

Fig. 1 shows the graphic dependence of the oxygen partial pressure for PdO decomposition on temperature, as described by Eq. (6). It is seen that both oxygen partial pressure and temperature can affect the stability of Pd or PdO. In ambient atmosphere where the oxygen partial pressure is 0.21 atm, PdO remains stable until temperature reaches 806 °C. This calculated value is the equilibrium decomposition temperature ($T_{d, eq.}$) of PdO in air and is in good agreement with the T_d obtained by TGA with an extremely low scan rate [20].

Fig. 2 shows the microstructures of the porous YSZ layer and the prepared Pd + YSZ cathode. The YSZ particles were well sintered after heat treatment at 1200 °C in air for 1 h, forming a porous YSZ scaffold (Fig. 2a). After Pd-impregnation, PdO particles smaller than 50 nm were formed and uniformly dispersed on the surface of the porous YSZ scaffold, constructing a functional composite cathode (Fig. 2b). Fig. 3 shows X-ray diffraction patterns of the Pd + YSZ cathode at various temperatures in air upon heating and cooling. The PdO phase in the cathode was stable at temperatures below 800 °C during heating, and the Pd phase appeared at temperatures above 800 °C and became the dominate species at 850 °C. According to this result, the decomposition temperature T_d of the nano-sized PdO particles supported on the YSZ substrate was under 800 °C
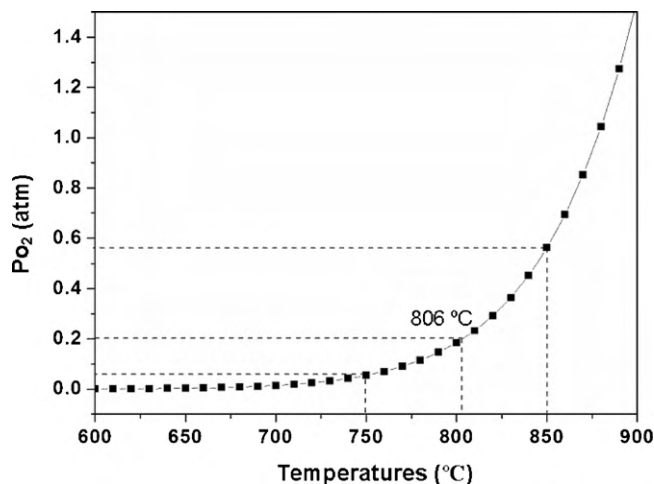

Fig. 1. Calculated relationship between equilibrium decomposition temperature of PdO and oxygen partial pressure.
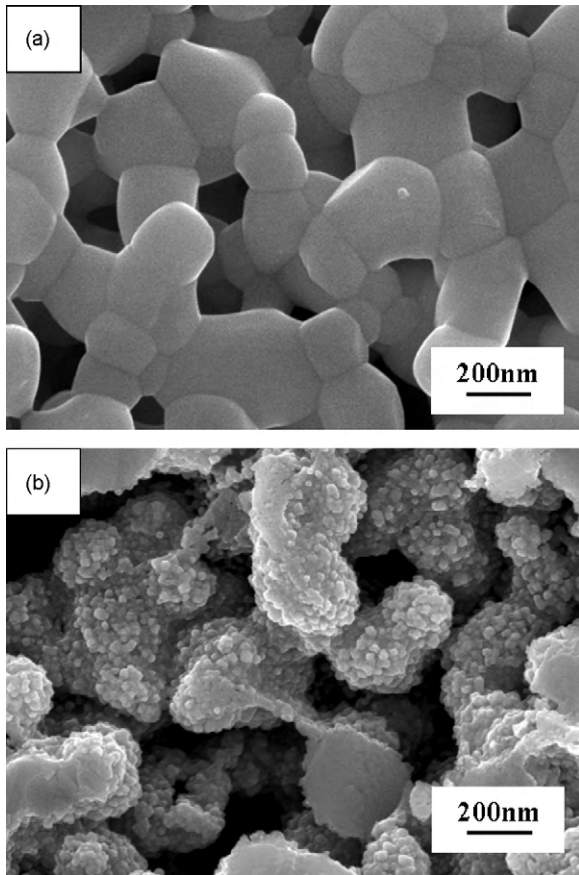
Fig. 2. Microstructures of the YSZ scaffold and the Pd + YSZ cathode prepared by solution impregnation.

during heating and significantly lower than that estimated from Eq. (6), thus suggesting that the T_d of the nano-sized PdO particles can be decreased from the equilibrium decomposition temperature $T_{d, eq}$ when they are supported on the oxide ion conductive YSZ substrate. In the cooling cycle from 900 °C, PdO started to reform at 750 °C and coexisted with Pd in the temperature range between 750 and 650 °C. As a matter of fact, such phenomena that the variation of the T_d temperature with supporting substrates and the coexistenc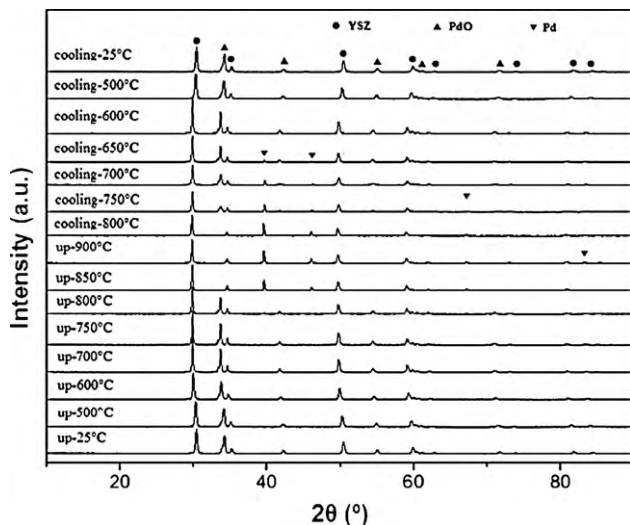e of Pd and PdO during cooling were reported previously [21–23]. The re-oxidation of Pd to PdO upon cooling is not simply a time–temperature rate process; a specific temperature is required. No PdO formation was observed at temperatures higher than the onset re-oxidation temperature T_r (between T_r and T_d), regardless the length of time held at the temperature. And the T_r is strongly affected by the nature of the supporting substrates. For the nano-sized Pd supported on CeO_2 substrate, the T_d temperature of PdO decreased to 775 °C and the T_r temperature was 730 °C, showing a hysteresis ($T_d - T_r$) of 45 °C that was much smaller than those supported on other non-ionic conductive substrates, such as Al_2O_3, undoped ZrO_2 and so on [21]. The co-existence of Pd and PdO was attributed to a skin of PdO formed on Pd particles [21,23]. The exchange of oxide ions between PdO and the ionic conductive substrate, such as the YSZ (present study) and CeO_2, may be responsible for the change of the T_d and T_r temperatures in terms of the equilibrium temperature of PdO and Pd. Detail mechanism still needs to be further understood.

3.2. Effect of oxygen partial pressure on cathode polarization resistance

Fig. 4 shows the electrochemical impedance spectra of the Pd + YSZ cathode under various oxygen partial pressures at 600 (Fig. 4a), 750 (Fig. 4b) and 850 °C (Fig. 4c), from which the area specific polarization resistance of the cathode R_E was derived and plotted as a function of oxygen partial pressure P_{O_2}, as shown in Fig. 4d. It is noticed that the R_E decreased linearly from 8.7 to 1.6 Ω cm^2 as the P_{O_2} increased from 0.001 to 1 atm at 600 °C. According to Fig. 1, the equilibrium oxygen partial pressure for PdO decomposition is 10^{-7} atm, which is considerably lower than 0.001 atm; thus it is reasonable to believe than the nano-sized PdO particles on the YSZ substrate was stable at 600 °C in the range of oxygen partial pressure used in the experiment. This is confirmed at one point by the high temperature XRD measurement (Fig. 3) that PdO was the only phase at 600 °C in air ($P_{O_2} = 0.21$ atm). Therefore, the decreased R_E with increasing P_{O_2} at 600 °C may be due to the enhanced O_2 adsorption on the PdO surfaces in O_2-richer atmospheres. In pure oxygen ($P_{O_2} = 1$ atm), the calculated $T_{d, eq}$ temperature is around 875 °C, which is slightly higher than the experimentally obtained value 851 °C reported in Ref. [20]. However, considering that PdO decomposes at much lower temperature than the thermodynamically equilibrium decomposition temperature as discussed above, it is expected that Pd remained stable in the Pd + YSZ cathode at 850 °C in the range of oxygen partial pressure between 0.001 and 1 atm; the dependence of the R_E on the P_{O_2}, i.e., the R_E decreases continuously at 850 °C from 0.8 to 0.02 Ω cm^2 as the P_{O_2} increases from 0.001 to 1 atm, can be understood by the enhanced O_2 access to the cathode surfaces at higher oxygen partial pressures. In the case of 750 °C, the R_E reached a minimum at around 0.03 atm of the P_{O_2}, beyond which the R_E increased with further increase in P_{O_2} to 1 atm. From Fig. 1, the equilibrium oxygen partial pressure for PdO decomposition is 0.054 atm at 750 °C, below and above which Pd and PdO should be the thermodynamically stable phase, respectively; and coexistence of the two phases could not be possible under thermodynamic equilibrium conditions. However, the R_E value of the cathode tested at 850 °C was higher than the one at 750 °C at $P_{O_2} = 0.01$ atm (0.35 Ω cm^2 at 850 °C vs. 0.2 Ω cm^2 at 750 °C in Fig. 4d), which is contradictory to the common knowledge that Pd becomes more electrocatalytically active at higher temperatures. Furthermore, the coexistence of Pd and PdO at 750 °C in air ($P_{O_2} = 0.21$) was confirmed by the high temperature XRD (Fig. 3). Thus these results indicate that Pd and PdO coexisted at least in the P_{O_2} range between 0.01 and 0.21 atm at 750 °C; and more PdO was formed as P_{O_2} increased. This discrepancy between the thermodynamic prediction of equilibrium phase and experimental observations suggests that the re-oxidation process of Pd
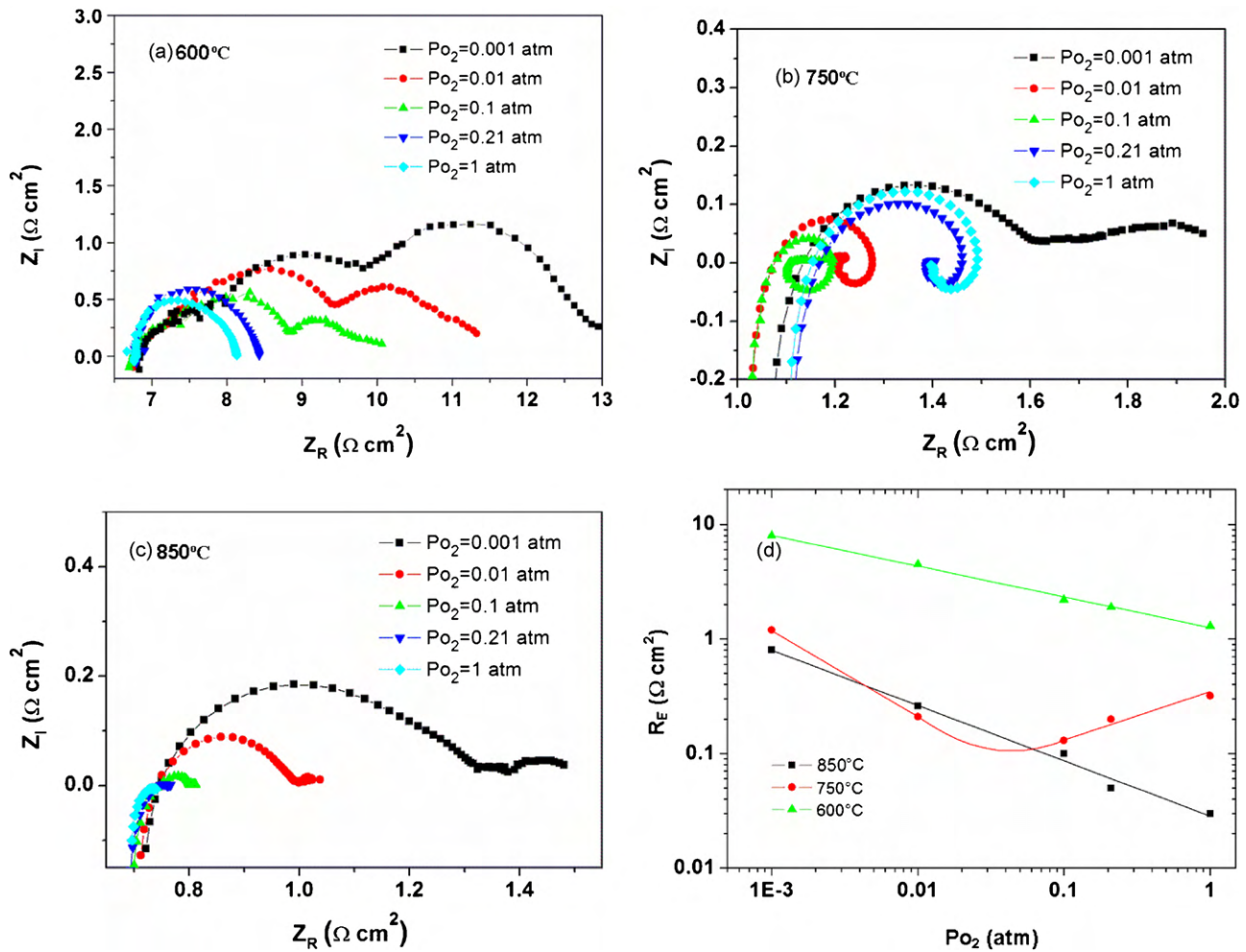

Fig. 3. XRD patterns of the Pd + YSZ cathode at various temperatures in air.

Fig. 4. Open circuit electrochemical impedance spectra of the Pd + YSZ cathode at (a) 600 °C, (b) 750 °C and (c) 850 °C under various oxygen partial pressures, and (d) dependence of the polarization resistance of the Pd + YSZ cathode on oxygen partial pressure at temperatures of 600, 750 and 850 °C.

is kinetically controlled. The fact that the R_E increased with P_{O_2} beyond the minimum indicates that excessive formation of PdO is detrimental to the oxygen reduction reaction in the Pd + YSZ cathode, due to its lower electrical conductivity.

In order to further understand the effect of oxygen partial pressure on the polarization resistance R_E of the Pd + YSZ cathodes at various temperatures, the impedance arcs in the first quadrant shown in Fig. 4 were deconvoluted into the high-frequency and low-frequency arcs by an equivalent circuit with a configuration of $LR_\Omega(R_{E1} - CPE_1)(R_{E2} - CPE_2)$ as shown in Fig. 5. In the equivalent circuit, the R_Ω is the overall ohmic resistance including those from the electrolyte, electrode and measuring leads, the L is an inductance element, the CPE1 and CPE2 are the constant phase elements, and the R_{E1} and R_{E2} are the resistances associated with the high- and low-frequency arcs, respectively. There is a general consensus in literature that the high-frequency arc is arisen from the ion-
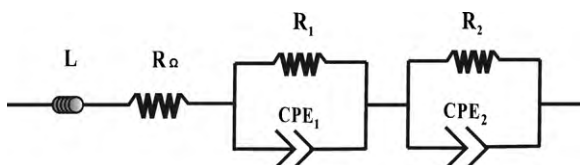
transfer process occurring at the electrode/electrolyte interfaces and the electron-transfer process accompanying with the oxygen reduction reaction; the low-frequency arc is considered the convoluted contributions of the adsorption and diffusion of oxygen at the gas–cathode interface and the surface diffusion of the intermediate oxygen species. Strong O_2 adsorption and dissociation are likely to cause this kind of low-frequency behavior (loop) according to our previous study [14], and further understanding of this phenomenon still needs to be established. The dependence of R_{E1} and R_{E2} on oxygen partial pressure is shown in Fig. 6, which is generally similar to that of the R_E shown in Fig. 4d. However, the values of R_{E2} at 850 °C are significantly higher than those at 750 °C in the P_{O_2} range from 0.01 to 0.21 atm, implying that the coexistence of Pd and PdO occurred in a wider range of P_{O_2} at 750 °C than expected above and considerably enhanced the processes of oxygen adsorption and surface diffusion associated with the reaction of oxygen reduction in the Pd + YSZ cathode.

It is known that the effectiveness of Pd as a catalyst to promote oxidation reactions of methane or other hydrocarbon fuels depends on its complex interactions with gaseous O_2 to form PdO or nonstoichiometric PdO_x [24,25]. If the following steps are assumed for oxygen reduction taking place in the Pd + YSZ cathode,
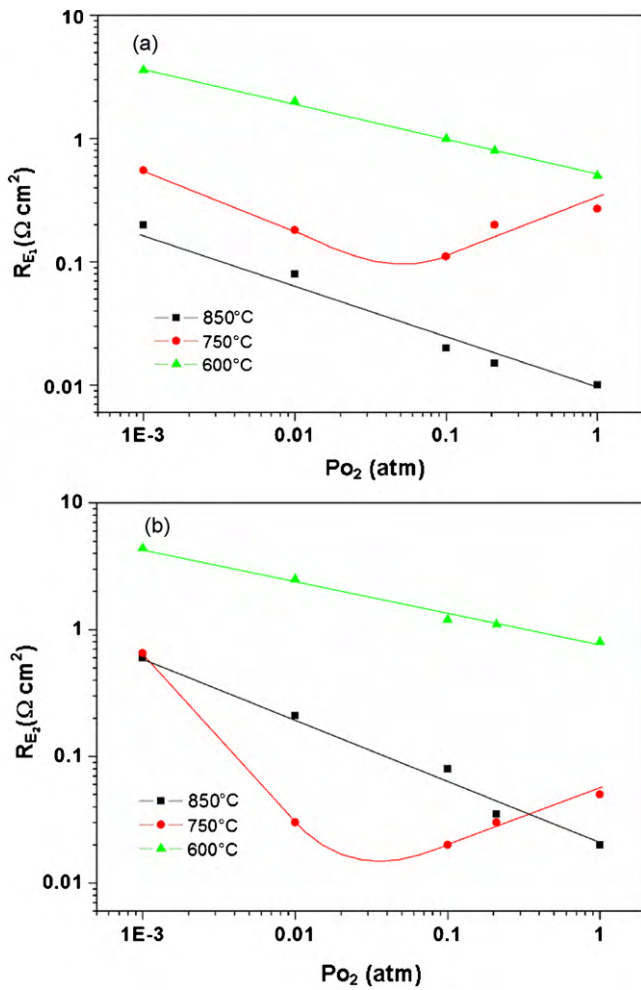

Fig. 5. Diagram of equivalent circuit which simulates the obtained impedance spectra shown in Fig. 4.

$$Pd + O_2 \rightarrow Pd\text{-}O_{2\,ads} \tag{7}$$

$$Pd\text{-}O_{2\,ads} \rightarrow Pd\text{-}O_{ads} \tag{8}$$

Fig. 6. Dependences of (a) R_{E1} and (b) R_{E2} on oxygen partial pressure at various temperatures between 600 and 850 °C.

$$Pd-O_{ads} \rightarrow PdO \qquad (9)$$

$$PdO + 2e^- + V_{O\,YSZ} \rightarrow Pd + O^{2-} \qquad (10)$$

where $O_{2\,ads}$ is the adsorbed oxygen molecules, O_{ads} is the adsorbed oxygen atoms, e^- is the electron obtained for reduction of PdO accompanied with an oxygen ion back-spilled simultaneously into an oxygen vacant site $V_{O\,YSZ}$ in the YSZ lattice (O^{2-}), then the coexistence of Pd and PdO is expected to facilitate the surface processes of oxygen reduction in the cathode by the inter-conversion between Pd and PdO.

3.3. Effect of Pd and PdO coexistence on activation energy of polarization resistance

Fig. 7 shows the representative electrochemical impedance spectra of the Pd + YSZ cathode at various temperatures between 600 and 850 °C in air under open circuit condition (Fig. 7a) and the corresponding polarization resistance R_E as a function of temperature (Fig. 7b). The semi-logarithmic plot of R_E against $1/T$ has three different slopes in the measured temperature range between 600 and 850 °C, corresponding three different electrocatalytic activation energies for the reaction of oxygen reduction according to the well-accepted relation [26]

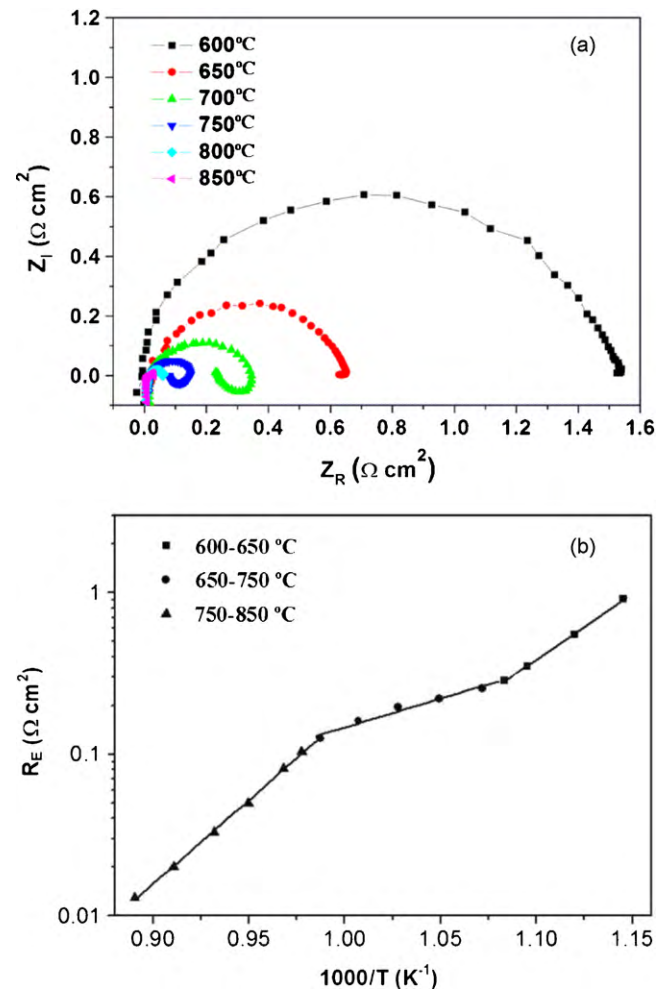$$\ln(\sigma) = -\frac{E_a}{RT} + \ln \sigma_0 \qquad (11)$$

Fig. 7. Open circuit electrochemical impedance spectra of the Pd + YSZ cathode at various temperatures between 600 and 850 °C (a) and the corresponding polarization resistance (R_E) as a function of temperature (b).

where $\sigma_0 \propto \frac{1}{R_E^0}$, $\sigma \propto \frac{1}{R_E}$, R_E^0 is a constant and E_a is the activation energy. In the temperature ranges from 850 to 750 °C and from 650 to 600 °C, Pd and PdO were stable in air, respectively, according to the results of high temperature XRD shown in Fig. 3; and the activation energies estimated were 198 and 155 kJ mol^{-1} correspondingly. In the temperature range between 750 and 650 °C, in which Pd and PdO coexisted, the activation energy was the lowest among the three activation energies with a value of 68 kJ mol^{-1}.

In a similar way to what have done in Section 3.2, the R_E here can also be deconvoluted into the R_{E1} and R_{E2} to separate the contributions of the charge-transfer and surface processes in the oxygen reduction reactions. From the dependence of R_{E1} and R_{E2} on testing temperatures shown in Fig. 8, it is observed once again that a much lower activation energy of 58 kJ mol^{-1} associated with the R_{E2} was obtained in the temperature range between 750 and 650 °C, compared to those obtained within the ranges of 850–750 °C (202 kJ mol^{-1}) and 650–600 °C (165 kJ mol^{-1}); and the activation energies associated with the R_{E1} were not dramatically different in various temperature ranges (147 kJ mol^{-1} between 850 and 750 °C, 106 kJ mol^{-1} between 750 and 650 °C, and 125 kJ mol^{-1} between 650 and 600 °C). This indicates that the coexistence of Pd and PdO promotes the thermally activated processes of oxygen adsorption and surface diffusion in the cathode, considerably decreases the activation energy associated with the resistance contributed by the adsorption and surface diffusion processes of oxygen.
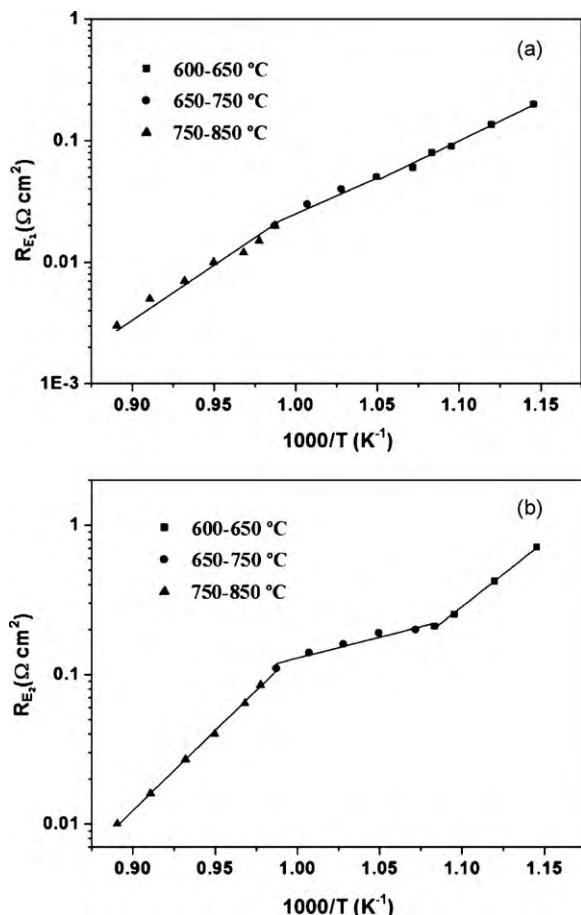
Fig. 8. Dependences of (a) R_{E1} and (b) R_{E2} of the Pd + YSZ cathode on temperature in air.

4. Conclusions

The redox behavior and electrocatalytic activity of the Pd + YSZ cathode were investigated and the following conclusions can be made:

1. PdO decomposes at 806 °C in air under thermodynamic equilibrium condition; the presence of YSZ substrate on which PdO particles are supported will change the redox temperatures in air and their dependence on oxygen partial pressure. In the Pd + YSZ cathode, PdO and Pd are stable in air at temperatures below 650 and above 800 °C, respectively; and Pd and PdO coexist in air in the temperature range of 650–750 °C.
2. The polarization resistance R_E decreases as P_{O_2} increases from 0.001 to 1 atm at both 600 and 850 °C, whereas it reaches a minimum in the same P_{O_2} range at 750 °C. This phenomenon is due to the coexistence of Pd and PdO in the Pd + YSZ cathode at 750 °C,

promoting the processes of oxygen adsorption and surface diffusion in the cathode.
3. The activation energy of polarization resistance of the Pd + YSZ cathode for oxygen reduction is 67.8 kJ mol^{-1} in the temperature range between 750 and 650 °C, which is the lowest compared to those obtained within the temperature ranges of 850–750 and 650–600 °C. This is attributed to the enhanced adsorption and surface diffusion of oxygen in the cathode.

Acknowledgements

References

[1] J.W. Fergus, Mater. Sci. Eng. A 397 (2005) 271–283.
[2] L.C. De Jonghe, C.P. Jacobson, S.J. Visco, Ann. Rev. Mater. Res. 33 (2003) 169–182.
[3] E. Ivers-Tiffee, A. Weber, D. Herbstritt, 7th International Conference on Electronic Ceramics and their Applications (ELECTROCERAMICS VII-2000), Portoroz, Slovenia, 2000, p. 1805.
[4] S.P. Jiang, Mater. Sci. Eng. A 418 (2006) 199.
[5] J.M. Vohs, R.J. Gorte, Adv. Mater. 21 (2009) 943–956.
[6] S.P. Jiang, Y.J. Leng, S.H. Chan, K.A. Khor, Electrochem. Solid-State Lett. 6 (2003) A67.
[7] S.P. Jiang, W. Wang, J. Electrochem. Soc. 152 (2006) A1398.
[8] J. Chen, F.L. Liang, B. Chi, J. Pu, S.P. Jiang, J. Li, J. Power Sources 194 (2009) 275–280.
[9] H. Uchida, S. Arisaka, M. Watanabe, Solid State Ionics 135 (2000) 347.
[10] H. Uchida, M. Yoshida, M. Watanabe, J. Electrochem. Soc. 146 (1999) 1.
[11] V.A.C. Haanappel, D. Rutenbeck, A. Mai, S. Uhlenbruck, D. Sebold, H. Wesemeyer, B. Röwekamp, C. Tropartz, F. Tietz, J. Power Sources 130 (2004) 119.
[12] M. Sahibzada, S.J. Benson, R.A. Rudkin, J.A. Kilner, Solid State Ionics 113–115 (1998) 285.
[13] W. Zhou, R. Ran, Z.P. Shao, R. Cai, W.Q. Jin, Electrochim. Acta 53 (2008) 4370–4380.
[14] F.L. Liang, J. Chen, J.L. Cheng, S.P. Jiang, T.M. He, J. Pu, J. Li, Electrochem. Commun. 10 (2008) 42–46.
[15] F.L. Liang, J. Chen, S.P. Jiang, B. Chi, J. Pu, J. Li, Electrochem. Solid State Lett. 11 (2008) B213–B216.
[16] F.L. Liang, J. Chen, S.P. Jiang, B. Chi, J. Pu, J. Li, Electrochem. Commun. 11 (2009) 1048–1051.
[17] F.L. Liang, J. Chen, S.P. Jiang, F.Z. Wang, B. Chi, J. Pu, J. Li, Fuel Cells 9 (2009) 636–642.
[18] J. Winker, P.V. Hendriksen, N. Bonanos, M. Mogensen, J. Electrochem. Soc. 145 (1998) 1184.
[19] D.L. Ye, J.H. Hu, Thermodynamic Manual of Inorganic Substances, 2nd edition, Metallurgical Industry Press, Beijing, 2002, pp. 810–815.
[20] H. Zhang, J. Gromek, G.W. Fernando, S. Boorse, H.L. Marcus, J. Phase Equilibr. 23 (2002) 246–248.
[21] R.J. Farrauto, J.K. Lampert, M.C. Hobson, E.M. Waterman, Appl. Catal. B 6 (1995) 263–270.
[22] P. Forzatti, G. Groppi, Catal. Today 54 (1999) 165–180.
[23] R.J. Farrauto, M. Hobson, T. Kennelly, E.M. Waterman, Appl. Catal. A 81 (1992) 227–237.
[24] M.M. Wolf, H.Y. Zhu, W.H. Green, G.S. Jackson, Appl. Catal. A 244 (2003) 323–340.
[25] S. Penner, P. Bera, S. Pedersen, L.T. Ngo, J.J.W. Harris, C.T. Campbell, J. Phys. Chem. B 110 (2006) 24577–24584.
[26] Y.M. Choi, M.C. Lin, M.L. Liu, J. Power Sources 195 (2010) 1441–1445.